

All product eigenstates in Heisenberg models from a graphical construction

Felix Gerken,^{1,2} Ingo Runkel,³ Christoph Schweigert,³ and Thore Posske^{1,2}

¹*I. Institut für Theoretische Physik, Universität Hamburg, Germany*

²*The Hamburg Centre for Ultrafast Imaging, Hamburg, Germany*

³*Fachbereich Mathematik, Universität Hamburg, Germany*

(Dated: October 23, 2023)

Recently, large degeneracy based on product eigenstates has been found in spin ladders, Kagome-like lattices, and motif magnetism, connected to spin liquids, anyonic phases, and quantum scars. We unify these systems by a complete classification of product eigenstates of Heisenberg XXZ Hamiltonians with Dzyaloshinskii-Moriya interaction on general graphs in the form of Kirchhoff rules for spin supercurrent. By this, we construct spin systems with extensive degree of degeneracy linked to exotic condensates which can be studied in atomic gases and quantum spin lattices.

Quantum spins interacting via the exchange interaction make up an archetypical many-body system, being exactly solvable only in certain limits, e.g., using the Bethe ansatz [1], Jordan-Wigner transformations [2, 3], or by selecting particular types of interactions [4]. One reason for this evasive behaviour is the high degree of entanglement, especially of the excited states, making analytic calculations challenging. Contrasting this, there recently have been a number of studies on product eigenstates in quantum spin systems that are connected to quantum many-body scars [5], which evade the eigenstate thermalization hypothesis [6, 7]. First examples were spin helices in 1D easy-plane quantum magnets [8–19] that have been dubbed phantom helices [12–14]. These states belong to a chiral reformulation of the Bethe ansatz at fine-tuned parameters of the one-dimensional XXZ quantum Heisenberg model where they consist of zero-energy quasi-particles. Phantom helices were experimentally observed in ultra cold atoms and generalized to higher dimensions [20]. Beyond one spatial dimension, product eigenstate can appear as ground states of Heisenberg models with carefully engineered magnetic fields manipulating the individual spins [11, 21, 22], In the vicinity of a critical point where the system shows macroscopic degeneracy, these systems carry a rich phase diagram including spin-liquid and broken symmetry phases. The product eigenstates were studied for their quantum scar properties [23] and generalized to lattices built from motifs, i.e., elementary building blocks, where they are ground states of frustrated lattices at a critical value of their exchange anisotropy [24], also further showing that product eigenstates exist in quasicrystalline Heisenberg magnets [25]. Product states are also a starting point for semi-classical and effective approaches to spin systems [26, 27]. E.g., product states have been used to elucidate the connection between classical and quantum skyrmions [28, 29], in particular, studies indicate that the central spin of quantum skyrmions could decouple in the ground state [30, 31].

In this manuscript, we give a procedure to completely classify product eigenstates in quantum Heisenberg models on general graphs. Our work unifies the approaches of

Refs. [9, 20, 24, 25] by supplying a graphical interpretation reminiscent of Kirchhoff’s law for electrical currents, which we use to solve the generally appearing coupled trigonometric equations [11, 21, 22]. According to these rules solving for product eigenstates amounts to choosing consistent flow patterns of spin supercurrent in the graph. In particular, we construct Heisenberg models with large degenerate eigenspaces containing a considerable amount of product eigenstates. To this end, our work builds on Cerezo et al. [21], who classified product eigenstates in spin-1/2 systems with non-uniform exchange interactions and magnetic fields in order to systematically engineer models with fully factorized ground states. We find that for models such as the square lattice with zig-zag edge the degeneracy scales exponentially in the size of the boundary of the system, and describe a suspension procedure to construct spin systems with a degeneracy of the product eigenstate subspace growing exponentially in system size. Other quantum spin models with extensive degeneracy have been recently proposed [24, 32–34]. We numerically find that the degeneracy of the energy eigenspace that accommodates the product eigenstates exceeds the dimension of the space spanned by the product eigenstates in accordance with earlier studies [9, 10, 24]. It is built up by additional non-product states that evade a simple description in terms of symmetries. This is consistent with results in spin ladders, where these additional states were linked to an anyonic condensate [10]. Our findings justify significant simplifications that have been made in Bethe ansatz approaches to XXZ quantum spin chains, including the existence of fully factorized pseudo vacuum [8], homogenous T - Q -relations for chains with non-diagonal boundary conditions [35], and the chiral reformulation of the ordinary Bethe ansatz [12–14]. By the general theory and the derived models with extensive degeneracies, spin product eigenstates and Heisenberg models on graphs hint at a crucial role of graph topology for entanglement, phase transitions and exact solubility that can potentially be observed in ultra cold atoms [20], Rydberg atoms [36, 37], qubit lattices and quantum computers [38–40], and chains of magnetic atoms on surfaces [41–43].

arXiv:2310.13158v1 [cond-mat.str-el] 19 Oct 2023

After completion of our work, we became aware of the recent Ref. [44], which touches on similar ideas.

Model & Method— We investigate quantum spins-1/2 on a simple undirected graph $\Lambda = (V, E)$, where V is the set of vertices and E is the set of edges. This excludes edges connecting the same pair of vertices and loops connecting a vertex to itself. We assign a spin-1/2 to each vertex. The dynamics are given in terms of a Hamiltonian constructed by assigning an XXZ spin-exchange interaction term and a Dzyaloshinskii-Moriya interaction (DMI) term to each edge.

$$H = \sum_{\{i,j\} \in E} \left[J (S_i^x S_j^x + S_i^y S_j^y) + \Delta S_i^z S_j^z - \kappa_{ij} D (S_i^x S_j^y - S_i^y S_j^x) \right], \quad (1)$$

with the exchange interaction J , the anisotropy Δ and the spin-1/2 operators $S_i^{x/y/z}$ acting on the spin at vertex i , $D \geq 0$ is the strength of the DMI and $\kappa_{ij} = -\kappa_{ji} = \pm 1$ is its sign.

The fully polarized states $|\uparrow \dots \uparrow\rangle$ and $|\downarrow \dots \downarrow\rangle$ are product eigenstates for all Hamiltonians of the form in Eq. (1). For finding additional product eigenstates, we follow the approach in [21] and insert the general ansatz for a product state

$$|\Psi(\vartheta, \varphi)\rangle = \bigotimes_{i \in V} \left(\cos\left(\frac{\vartheta_i}{2}\right) e^{-i\frac{\varphi_i}{2}} |\uparrow\rangle_i + \sin\left(\frac{\vartheta_i}{2}\right) e^{i\frac{\varphi_i}{2}} |\downarrow\rangle_i \right) \quad (2)$$

into the eigenvalue equation for H . Here, $\vartheta = (\vartheta_1, \dots, \vartheta_{|V|})$ are the angles relative to the hard-axis z and $\varphi = (\varphi_1, \dots, \varphi_{|V|})$ are the angles in the easy-plane x - y taking values $\vartheta_i \in (0, \pi)$ and $\varphi_i \in [0, 2\pi)$. The eigenvalue problem $H|\Psi(\vartheta, \varphi)\rangle = \varepsilon(\vartheta, \varphi)|\Psi(\vartheta, \varphi)\rangle$ yields a coupled set of trigonometric equations constraining the angles, ϑ and φ , see [21] and the Supplemental Material [45].

Results— Among the constraining equations there are pairs, one for each edge, that constrain the relative angles of adjacent spins. The remaining equations can then be condensed to very few rules that characterize all product eigenstates, which we discuss in the following. For easy-axis magnetism, $\Delta^2 > J^2 + D^2$, we find that the only product eigenstates are $|\uparrow \dots \uparrow\rangle$ and $|\downarrow \dots \downarrow\rangle$ [45]. Additional interactions such as magnetic fields are required to obtain further product eigenstates in this case. For easy-plane magnetism, $\Delta^2 \leq J^2 + D^2$, we develop a graphical interpretation of the constraints for the product eigenstates. First, the polar angle of the spins is constant $\vartheta_j = \Theta$, corresponding to a canted spin configuration. Secondly, the exchange interactions constrain the azimuthal angles of adjacent spins to $\varphi_i - \varphi_j = \kappa_{ij}\delta + \sigma_{ij}\gamma$, where the DMI defines a bias angle $\delta = \arctan(D/J)$ and the anisotropy determines the anisotropy angle $\gamma = \arccos(\Delta/\sqrt{J^2 + D^2})$. Here, each edge has a binary degree of freedom with $\sigma_{ij} = -\sigma_{ji} = \pm 1$. As a consequence,

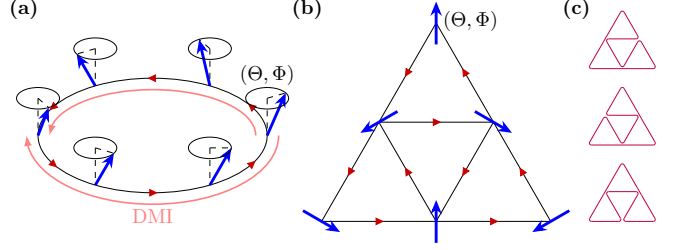


FIG. 1. Graphical solution to the product eigenstate problem, shown by a Heisenberg model on two graphs with spins at the vertices (blue arrows depicting spin expectation values $\langle \mathbf{S} \rangle = (\langle S^x \rangle, \langle S^y \rangle, \langle S^z \rangle)^T$) and edges denoting the exchange interaction and the DMI, see Eq.(1). The change of the azimuthal angle along an edge can take the values $\kappa_{ij}\delta + \sigma_{ij}\gamma$. The sign σ_{ij} is indicated by the direction of the red arrows. (a) Spin chain with anisotropy and bias angles $\gamma = \pi/3$ and $\delta = \pi/6$. The signs of the DMI κ_{ij} are indicated by rose arrows giving bias angles of $+\delta$ (top half) and $-\delta$ (bottom half). The reference angles are $\Theta = \pi/3$ and $\Phi = \pi/6$. (b) Triangular lattice with $\gamma = 2\pi/3$ and $D = 0$ with a product eigenstate and its Kirchhoff orientation (red arrows) and its reference angles $\Theta = \Phi = \pi/2$ (top view). (c) Euler circuit for the triangular lattice in (b).

the degrees of freedom of the product eigenstates are two continuous global angles Θ and Φ , fixing the orientation of a reference spin $\vartheta_1 \equiv \Theta$ and $\varphi_1 \equiv \Phi$, as well as the discrete degree of freedom of choosing the signs σ_{ij} . The latter degree of freedom corresponds to choosing an orientation of the underlying graph described by assigning a direction to an edge $\{i, j\}$, that we depict by an arrow pointing towards vertex i if $\varphi_i - \varphi_j = \kappa_{ij}\delta + \gamma$ and in the other direction if $\varphi_i - \varphi_j = \kappa_{ij}\delta - \gamma$. The choice of orientation σ has to be commensurate with two rules reminiscent of Kirchhoff's laws for electrical currents:

Vertex rule: At each vertex i , the number of ingoing arrows equals the number of outgoing arrows. $\sum_{\{i,j\} \in E} \sigma_{ij} = 0$, depicted by, e.g.,

Circuit rule: The change of the azimuthal angle along a circuit $\Gamma \subset E$ in the graph must consistently be an integer multiple of 2π . $\sum_{\{i,j\} \in \Gamma} (\kappa_{ij}\delta + \sigma_{ij}\gamma) \equiv 0 \pmod{2\pi}$, depicted by, e.g.,

There are two special cases for $\Delta^2 = J^2 + D^2$. For $\gamma = 0$, the σ is not well-defined since $-\gamma = \gamma \pmod{2\pi}$. There are only the two trivial product eigenstates. For $\gamma = \pi$, σ is not well-defined either. In this case, a non-trivial product eigenstate exists if the circuit rule can be fulfilled. The vertex rule is not to be confused with Gauß' law in lattice gauge theories [46]. In physical terms, the vertex rule corresponds to the local conservation of the z -component of the spin, i.e., compensating spin supercurrents C_{ij} at

vertex i

$$\langle \dot{S}_i^z \rangle = \sum_{\{i,j\} \in E} C_{ij} = \frac{\sin^2(\Theta) \sin(\gamma) \hbar^2 J}{4 \cos(\delta)} \sum_{\{i,j\} \in E} \sigma_{ij} = 0 \quad (3)$$

In accordance with this interpretation the vertex rule can be extended to Hamiltonians including local magnetic fields $\mathbf{B}_i \mathbf{S}_i$ such that the field acts as source and sink terms compensating the difference between ingoing and outgoing arrows [45]. Including DMI allows for modifying the circuit rule, while fine-tuned magnetic fields would soften the vertex rule.

An orientation σ that satisfies the vertex rule at each vertex is an Euler orientation. These have the property that there is at least one closed trail that travels each edge in the direction of the Euler orientation exactly once [47]. To simplify terminology, we refer to an Euler orientation fulfilling the circuit rule for a Hamiltonian in Eq. (1) as a *Kirchhoff orientation* of a *Kirchhoff graph*. This should not be confused with the notion of Kirchhoff graphs in the context of reaction route graphs [48, 49]. Any product state commensurate with the Kirchhoff rules has an appealing interpretation: When we unravel a closed trail as above, the state looks like a helix with local pitch angles γ that are distorted by local bias angles $\pm\delta$ in presence of DMI. In this sense, the product states are a natural extension of the recently discovered phantom helices [12–14] to arbitrary graphs. Remarkably, all product eigenstates of Eq. (1) have the same energy independent of DMI

$$\varepsilon = \hbar^2 \Delta |E|/4. \quad (4)$$

In the following, we refer to the space of all eigenstates with the same energy as the product eigenstates as the ε -space and the subspace spanned by the product eigenstates as product eigenspace. An upper bound for the product eigenspace dimension is given by

$$2 + \sum_{k=1}^{|V|-1} \min \left(|\sigma|, \binom{|V|}{k} \right), \quad (5)$$

where $|\sigma|$ is the number of Kirchhoff orientations. For $\gamma = 0$ and $\gamma = \pi$, we set $|\sigma| = 1$. This bound follows from considering the projections on the $|V|+1$ eigenspaces P_k , $k \in \{0, \dots, |V|\}$, of the symmetry operator $\sum_{i \in V} S_i^z$. A product eigenstate $|\Psi(\Theta, \Phi)\rangle$ with $\Theta \neq 0, \pi$ gives $|V|+1$ orthogonal eigenstates $P_k |\Psi(\Theta, \Phi)\rangle$ of the same energy. Given another non-trivial product eigenstate $|\Psi(\Theta', \Phi')\rangle$ with the same Kirchhoff orientation, the projected states differ merely by a non-zero factor, i.e., $P_k |\Psi(\Theta', \Phi')\rangle \sim P_k |\Psi(\Theta, \Phi)\rangle$. So, for any projector P_k , the image of the product eigenspace under this projector contains at most $|\sigma|$ linear independent vectors and is further bounded by the dimension of $\text{im}(P_k)$ which is $|V|$ choose k . Since the trivial product eigenstates $|\uparrow \dots \uparrow\rangle$ and $|\downarrow \dots \downarrow\rangle$ span the spaces $\text{im}(P_0)$ and $\text{im}(P_{|V|})$ the dimension is always at

least 2. For graphs with vanishing DMI and anisotropy angle $\gamma = \pi/(2n)$, n a positive integer, we prove that the number of Kirchhoff orientations $|\sigma|$ gives a lower bound on the product eigenspace degeneracy [45]. In this case, the dimension of the product eigenspace has both an upper and a lower bound linear in $|\sigma|$.

A physical interpretation of the product eigenspace can be given in terms of delocalized spin-flips. For a given Kirchhoff orientation, the span of the product eigenstates $|\Psi(\Theta, \Phi)\rangle$ is generated by states $R^{(n)} |\Psi(\pi/2, \Phi_0)\rangle$ consisting of n delocalized spin-flips with $0 \leq n \leq |V|$ and some fixed Φ_0 . R is defined as

$$R^{(n)} = \sum_{\{i_1, \dots, i_n\} \subset V} P_{i_1} \dots P_{i_n} \quad (6)$$

where P_i acts on a product eigenstate as in Eq. (2) by $\vartheta_i \mapsto \pi - \vartheta_i$ and $\varphi_i \mapsto \varphi_i - \pi$ and hence flipping the expectation value of its i^{th} spin, i.e., $\langle \mathbf{S}_i \rangle \mapsto -\langle \mathbf{S}_i \rangle$. We set $R^{(0)} \equiv 1$ and note that $R^{(n)} = 0$ for $n > |V|$ since the sum is empty. These states can be expressed in terms of a linear combination of derivatives of $|\Psi(\Theta, \Phi)\rangle$ with respect to Θ and Φ which are also eigenstates of H , given by Eq. (4),

$$\partial_{\Theta} |\Psi(\Theta, \Phi)\rangle = \frac{i}{2} \sum_{i \in V} P_i |\Psi(\Theta, \Phi)\rangle, \quad (7)$$

$$\partial_{\Phi} |\Psi(\Theta, \Phi)\rangle = \frac{1}{2} \sum_{i \in V} e^{-\frac{i}{\hbar} \pi S_i^z} |\Psi(\Theta, \Phi)\rangle, \quad (8)$$

and at $\Theta = \pi/2$, $\Phi = \Phi_0$ the derivatives can be conversely expressed in terms of the spin-flip states. The delocalized spin-flip states span the product eigenspace since the eigenspace generated by all product eigenstates and the eigenspace generated by the derivatives at the angles $\Theta = \pi/2$ and $\Phi = \Phi_0$ are the same. This is because on the one hand every product state has a converging Taylor expansion in Θ and Φ (see Eq. (2) with $\vartheta_1 = \Theta$, $\varphi_1 = \Phi$ and the other angles according to the Kirchhoff orientation), and on the other hand, every derivative can be expressed as the limit of a differential quotient of product eigenstates.

Applications— We next discuss well-known systems without DMI and their product eigenstates in our graphical framework. In 1D, spin helices are well-studied product eigenstates. For vanishing DMI, a periodic spin chain with N sites has two Kirchhoff orientations if the periodic closure condition $\gamma N \equiv 0 \pmod{2\pi}$ [11, 12] is fulfilled, corresponding to two helices with opposite helicity. In absence of DMI, inverting the direction of arrows in a Kirchhoff orientation generally yields another permissible orientation. Numerically, we find that the product eigenstates in the circular chain generate a degeneracy linear in the chain length N [45]. However, the product eigenstates do not span the entire ε -space for all choices of permissible γ and N . The triangular lattice depicted

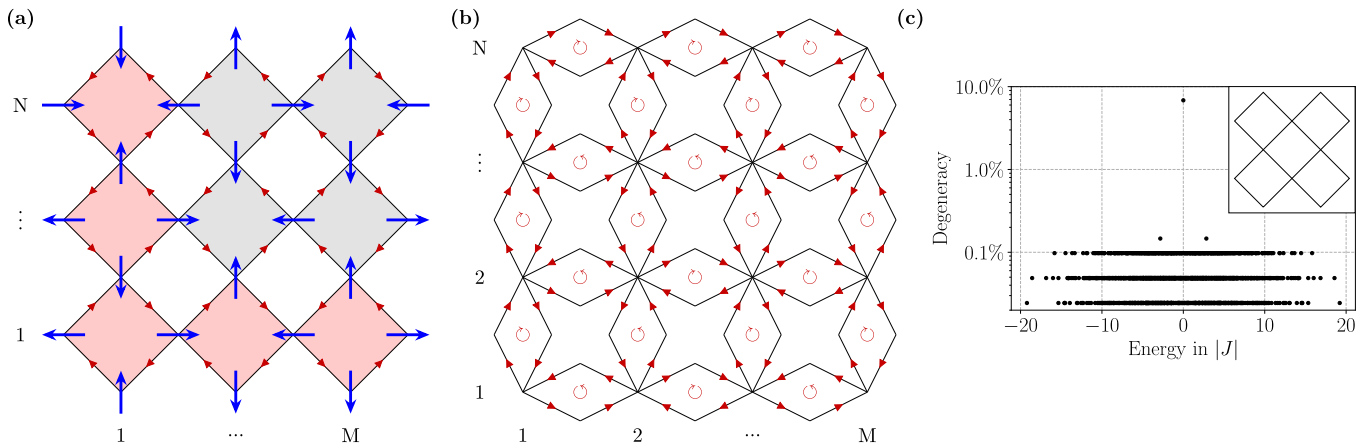


FIG. 2. **(a)** XX model ($\Delta = D = 0$) on a square lattice with zig-zag edge and its product eigenstates. Fixing $\Theta = \pi/2$, the spins align row- and column-wise in a Néel pattern determined by the boundary spins for the N rows and M columns resulting in 2^{N+M-1} Kirchoff orientations. **(b)** The replacement of edges by “diamond” squares allows for a number of Kirchoff orientations that grows exponentially in the number of diamonds with a lower bound of $2^{2NM+N+M}$ Kirchoff orientations. **(c)** Degeneracy of the eigenspaces of the XX model on a square lattice, see inset, as a fraction of the total Hilbert space dimension. The eigenspace that accommodates the product eigenstates has energy zero commensurate with Eq. (4), and is two orders of magnitude more degenerate than typical eigenspaces.

in Fig. 1b also allows for two different choices of Kirchoff orientations independent of the system size whose product eigenstates are part of the ground space [24]. More generally for graphs made up of triangular motifs, the choice of a Kirchoff orientation is equivalent to a three-coloring of the graph which has been used to study product eigenstates in such systems [24]. For the kagome lattice, the abundance of three-colorings yields an extensively degenerate ground space, i.e., for this family of systems, the degeneracy grows exponentially in the number of spins. We proceed with constructing novel lattices with macroscopic degeneracy. We first detail the square lattice with zig-zag boundary conditions, see Fig. 2a, where the number of Kirchoff orientations increases exponentially with the size of the system’s boundary. To that end, we consider the XX model, i.e., $\Delta = D = 0$ in Eq. (1), corresponding to $\gamma = \pi/4$. We find that the boundaries of this model enforce a checkerboard pattern, c.f. Fig. 2a, where arrows along the colored plaquettes of the checkerboard form a vortex configuration going around the adjacent gray or rose plaquette. Specifying the M vortices at the bottom and the $N - 1$ vortices at the left boundary (rose in Fig. 2a) fully determines the inner ones (gray and white). Hence, the number of Kirchoff orientations is 2^{N+M-1} , i.e., grows exponentially with the size of the boundary [45]. On the level of the individual spins, fixing the spin in the lower left corner to point along the x -axis, the degrees of freedom are choosing the leftmost spins pointing either in the $(+x)$ - or $(-x)$ -direction and the bottom spins pointing either in the $(+y)$ - or $(-y)$ -direction. The remaining spins will anti-align with their neighbors along each column and row of spins, see Fig. 2a. We find numerically that the

dimension of the space spanned by product eigenstates is consistent with $(MN + 1)2^{N+M}$. In the special case of $N = 1$ or $M = 1$, the degeneracy scales exponentially with the system’s size, and is hence an extensive quantity. Such diamond chains have been studied among other reasons for their degeneracy in the context of exactly solvable systems [50, 51] and spin ladders [52].

We find that systems with an extensively degenerate eigenspace of product eigenstates can be engineered by a suspension procedure similar to earlier ideas of building graphs from smaller motifs [24, 25]. For a given graph, we replace each edge of the graph by a subgraph, e.g., for the square lattice, we substitute the edges by a single diamond square oriented clockwise or anticlockwise, see Fig. 2b. The construction respects the vertex and the circuit rule and yields extensive degeneracy exponential in the number of independently oriented diamonds, which results in a lower bound of $2^{2NM+N+M}$.

Degeneracy & intrinsic structure of ε -spaces— In general, the degeneracy of the product eigenspace exceeds the number of possible Kirchoff orientations. We analyze the ε -space for the square lattice and the diamond chain. We numerically confirm for $(N, M) = (1, 1), (1, 2), (1, 3),$ and $(2, 2)$ that the ε -space is the most degenerate eigenspace, see [45]. Typically the eigenspaces are one or two orders of magnitude more degenerate than all other eigenspaces, making up a large share of the total Hilbert space dimension, see Fig. 2c. Additional degeneracy stems from states with non-vanishing entanglement entropy. In special cases in 1D, these have been associated with anyonic condensates [9] or spin liquid phases [24].

Discussion— We developed the complete classification scheme of product eigenstates of Heisenberg Hamiltonians with XXZ exchange interactions and DMI by Kirchhoff’s rules for the underlying graph. Some graphs feature associated Kirchhoff orientations in abundance. They possess large degenerate eigenspaces with zero-energy delocalized spin-flip excitations and additional non-product states associated to anyonic statistics in special systems. We thereby give a concrete example for a fundamental property connecting graph topology, degeneracy, and entanglement. Further, we numerically find additional degeneracy for the same energy as the product eigenstates that coincides with the fulfillment of Kirchhoff’s rules. The degeneracy is reduced when moving away from the critical value of γ [45]. The singular nature of the degeneracy of the eigenspace accommodating the product eigenstates excludes a simple explanation of this phenomenon by the natural symmetries of the model. The considered graphs in general describe quantum spin systems of any dimension. As such, our study could be a step towards a partial solutions of XXZ Heisenberg models in more than one dimension, at least for a critical value of γ . Possibly by making use of the one-dimensional Euler circles reminiscent of trails for Jordan-Wigner strings [2, 3, 53] and bosonization approaches [54].

FG and TP thank Oleg Tchernyshyov for helpful discussions. FG acknowledges funding by the Cluster of Excellence “CUI: Advanced Imaging of Matter” of the Deutsche Forschungsgemeinschaft (DFG) – EXC 2056 – project ID 390715994. IR and CS are partially supported by the Deutsche Forschungsgemeinschaft via the Cluster of Excellence EXC 2121 “Quantum Universe” - 390833306. TP acknowledges funding by the DFG (German Science Foundation) project number 420120155 and the European Union (ERC, QUANTWIST, project number 101039098). Views and opinions expressed are however those of the authors only and do not necessarily reflect those of the European Union or the European Research Council. Neither the European Union nor the granting authority can be held responsible for them.

[1] V. E. Korepin, N. M. Bogoliubov, and A. G. Izergin, *Quantum Inverse Scattering Method and Correlation Functions* (Cambridge University Press, Cambridge, 1993).

[2] P. Jordan and E. Wigner, Über das Paulische Äquivalenzverbot, *Z. Phys.* **47**, 631 (1928).

[3] E. Lieb, T. Schultz, and D. Mattis, Two soluble models of an antiferromagnetic chain, *Ann. Phys.* **16**, 407 (1961).

[4] A. Kitaev, Anyons in an exactly solved model and beyond, *Ann. Phys.* **321**, 2 (2006).

[5] S. Moudgalya, B. A. Bernevig, and N. Regnault, Quantum many-body scars and Hilbert space fragmentation:

a review of exact results, *Rep. Prog. Phys.* **85**, 086501 (2022).

[6] J. M. Deutsch, Quantum statistical mechanics in a closed system, *Phys. Rev. A* **43**, 2046 (1991).

[7] M. Srednicki, Chaos and quantum thermalization, *Phys. Rev. E* **50**, 888 (1994).

[8] J. Cao, H. Q. Lin, K. J. Shi, and Y. Wang, Exact solution of XXZ spin chain with unparallel boundary fields, *Nucl. Phys. B* **663**, 487 (2003).

[9] C. D. Batista, Canted spiral: An exact ground state of XXZ zigzag spin ladders, *Phys. Rev. B* **80**, 180406 (2009).

[10] C. D. Batista and R. D. Somma, Condensation of anyons in frustrated quantum magnets, *Phys. Rev. Lett.* **109**, 227203 (2012).

[11] M. Cerezo, R. Rossignoli, and N. Canosa, Factorization in spin systems under general fields and separable ground-state engineering, *Phys. Rev. A* **94**, 042335 (2016).

[12] V. Popkov, X. Zhang, and A. Klümper, Phantom Bethe excitations and spin helix eigenstates in integrable periodic and open spin chains, *Phys. Rev. B* **104**, L081410 (2021).

[13] X. Zhang, A. Klümper, and V. Popkov, Phantom Bethe roots in the integrable open spin- $\frac{1}{2}$ XXZ chain, *Phys. Rev. B* **103**, 115435 (2021).

[14] X. Zhang, A. Klümper, and V. Popkov, Chiral coordinate Bethe ansatz for phantom eigenstates in the open XXZ spin- $\frac{1}{2}$ chain, *Phys. Rev. B* **104**, 195409 (2021).

[15] X. Zhang, A. Klümper, and V. Popkov, Invariant subspaces and elliptic spin-helix states in the integrable open spin- $\frac{1}{2}$ XYZ chain, *Phys. Rev. B* **106**, 075406 (2022).

[16] E. S. Ma, K. L. Zhang, and Z. Song, Steady helix states in a resonant XXZ Heisenberg model with Dzyaloshinskii-Moriya interaction, *Phys. Rev. B* **106**, 245122 (2022).

[17] V. Popkov, M. Žnidarič, and X. Zhang, Universality in the relaxation of spin helices under XXZ spin-chain dynamics, *Phys. Rev. B* **107**, 235408 (2023).

[18] S. Kühn, F. Gerken, L. Funcke, T. Hartung, P. Stornati, K. Jansen, and T. Posske, Quantum spin helices more stable than the ground state: Onset of helical protection, *Phys. Rev. B* **107**, 214422 (2023).

[19] Y. B. Shi and Z. Song, Robust unidirectional phantom helix states in the XXZ heisenberg model with Dzyaloshinskii-Moriya interaction, *Phys. Rev. B* **108**, 085108 (2023).

[20] P. N. Jepsen, Y. K. E. Lee, H. Lin, I. Dimitrova, Y. Margalit, W. W. Ho, and W. Ketterle, Long-lived phantom helix states in Heisenberg quantum magnets, *Nat. Phys.* **18**, 899 (2022).

[21] M. Cerezo, R. Rossignoli, and N. Canosa, Nontransverse factorizing fields and entanglement in finite spin systems, *Phys. Rev. B* **92**, 224422 (2015).

[22] M. Cerezo, R. Rossignoli, N. Canosa, and E. Ríos, Factorization and criticality in finite XXZ systems of arbitrary spin, *Phys. Rev. Lett.* **119**, 220605 (2017).

[23] K. Lee, R. Melendrez, A. Pal, and H. J. Changlani, Exact three-colored quantum scars from geometric frustration, *Phys. Rev. B* **101**, 241111 (2020).

[24] H. J. Changlani, D. Kochkov, K. Kumar, B. K. Clark, and E. Fradkin, Macroscopically degenerate exactly solvable point in the spin-1/2 kagome quantum antiferromagnet, *Phys. Rev. Lett.* **120**, 117202 (2018).

[25] E. Chertkov and B. K. Clark, Motif magnetism and quantum many-body scars, *Phys. Rev. B* **104**, 104410 (2021).

- [26] S. K. Kim and Y. Tserkovnyak, Topological effects on quantum phase slips in superfluid spin transport, *Phys. Rev. Lett.* **116**, 127201 (2016).
- [27] Y. Tserkovnyak, J. Zou, S. K. Kim, and S. Takei, Quantum hydrodynamics of spin winding, *Phys. Rev. B* **102**, 224433 (2020).
- [28] R. Takashima, H. Ishizuka, and L. Balents, Quantum skyrmions in two-dimensional chiral magnets, *Phys. Rev. B* **94**, 1 (2016).
- [29] O. M. Sotnikov, E. A. Stepanov, M. I. Katsnelson, F. Mila, and V. V. Mazurenko, Reconstruction of classical skyrmions from Anderson towers: quantum Darwinism in action (2022), arXiv:2210.03922 [quant-ph].
- [30] A. Haller, S. Groenendijk, A. Habibi, A. Michels, and T. L. Schmidt, Quantum skyrmion lattices in Heisenberg ferromagnets, *Phys. Rev. Res.* **4**, 043113 (2022).
- [31] A. Joshi, R. Peters, and T. Posske, Ground state properties of quantum skyrmions described by neural network quantum states, *Phys. Rev. B* **108**, 094410 (2023).
- [32] G. Palle and O. Benton, Exactly solvable spin- $\frac{1}{2}$ XYZ models with highly degenerate partially ordered ground states, *Phys. Rev. B* **103**, 214428 (2021).
- [33] D. V. Dmitriev and V. Y. Krivnov, Two-dimensional spin models with macroscopic degeneracy, *J. Phys.: Cond. Mat.* **33**, 435802 (2021).
- [34] Z. Nussinov and G. Ortiz, Theorem on extensive spectral degeneracy for systems with rigid higher symmetries in general dimensions, *Phys. Rev. B* **107**, 045109 (2023).
- [35] R. Murgan and R. I. Nepomechie, Generalized T - Q relations and the open XXZ chain, *J. Stat. Mech.* **0508**, P08002 (2005).
- [36] C. Chen, G. Bornet, M. Bintz, G. Emperauger, L. Leclerc, V. S. Liu, P. Scholl, D. Barredo, J. Hauschild, S. Chatterjee, M. Schuler, A. M. Läuchli, M. P. Zaletel, T. Lahaye, N. Y. Yao, and A. Browaeys, Continuous symmetry breaking in a two-dimensional Rydberg array, *Nature* **616**, 691 (2023).
- [37] B. Sbierski, M. Bintz, S. Chatterjee, M. Schuler, N. Y. Yao, and L. Pollet, Magnetism in the two-dimensional dipolar XY model (2023), arXiv:2305.03673 [cond-mat.quant-gas].
- [38] A. D. King, J. Carrasquilla, J. Raymond, I. Ozfidan, E. Andriyash, A. Berkley, M. Reis, T. Lanting, R. Harris, F. Altomare, K. Boothby, P. I. Bunyk, C. Enderud, A. Fréchet, E. Hoskinson, N. Ladizinsky, T. Oh, G. Poulin-Lamarre, C. Rich, Y. Sato, A. Y. Smirnov, L. J. Swenson, M. H. Volkmann, J. Whittaker, J. Yao, E. Ladizinsky, M. W. Johnson, J. Hilton, and M. H. Amin, Observation of topological phenomena in a programmable lattice of 1,800 qubits, *Nature* **560**, 456 (2018).
- [39] F. Tacchino, A. Chiesa, S. Carretta, and D. Gerace, Quantum computers as universal quantum simulators: State-of-the-art and perspectives, *Adv. Quant. Tech.* **3**, 1900052 (2020).
- [40] J. S. Van Dyke, E. Barnes, S. E. Economou, and R. I. Nepomechie, Preparing exact eigenstates of the open XXZ chain on a quantum computer, *J. Phys. A: Math. Theor.* **55**, 055301 (2022).
- [41] A. A. Khajetoorians, J. Wiebe, B. Chilian, and R. Wiesendanger, Realizing all-spin-based logic operations atom by atom, *Science* **332**, 1062 (2011).
- [42] A. A. Khajetoorians, B. Baxevanis, C. Hübner, T. Schlenk, S. Krause, T. O. Wehling, S. Lounis, A. Lichtenstein, D. Pfannkuche, J. Wiebe, and R. Wiesendanger, Current-driven spin dynamics of artificially constructed quantum magnets, *Science* **339**, 55 (2013).
- [43] Y. Chen, Y. Bae, and A. J. Heinrich, Harnessing the quantum behavior of spins on surfaces, *Adv. Mater.* **35**, 2107534 (2023).
- [44] C. H. Zhang, Y. B. Shi, and Z. Song, Generalized phantom helix states in quantum spin graphs (2023), arXiv:2310.11786 [quant-ph].
- [45] See Supplemental Material at [URL will be inserted by the publisher] for details.
- [46] S. Chandrasekharan and U.-J. Wiese, Quantum link models: A discrete approach to gauge theories, *Nuclear Physics B* **492**, 455 (1997).
- [47] L. Euler, Solutio problematis ad geometriam situs pertinentis, *Commentarii academiae scientiarum Petropolitanae* **8**, 128 (1741).
- [48] J. D. Fehribach, Vector-space methods and Kirchhoff graphs for reaction networks, *SIAM J. Appl. Math.* **70**, 543 (2009).
- [49] I. Fishtik, C. A. Callaghan, and R. Datta, Reaction route graphs. I. Theory and algorithm, *J. Phys. Chem. B* **108**, 5671 (2004).
- [50] B. Sutherland and B. S. Shastry, Exact solution of a large class of interacting quantum systems exhibiting ground state singularities, *J. Stat. Phys.* **33**, 477 (1983).
- [51] K. Takano, K. Kubo, and H. Sakamoto, Ground states with cluster structures in a frustrated Heisenberg chain, *J. Phys.: Cond. Mat.* **8**, 6405 (1996).
- [52] M. Ishii, H. Tanaka, M. Hori, H. Uekusa, Y. Ohashi, K. Tatani, Y. Narumi, and K. Kindo, Gapped ground state in the spin- $\frac{1}{2}$ trimer chain system $\text{Cu}_3\text{Cl}_6(\text{H}_2\text{O})_2 \cdot 2\text{H}_8\text{C}_4\text{SO}_2$, *J. Phys. Soc. Jpn.* **69**, 340 (2000).
- [53] E. Fradkin, Jordan-Wigner transformation for quantum-spin systems in two dimensions and fractional statistics, *Phys. Rev. Lett.* **63**, 322 (1989).
- [54] J. von Delft and H. Schoeller, Bosonization for beginners — refermionization for experts, *Ann. Phys.* **510**, 225 (1998).

Explicit product ansatz

We give detailed expressions for the equations defining the product eigenstates in the main text. To this end, we consider a more general Hamiltonian including XXZ exchange interaction, DMI and on-site magnetic fields.

$$H = \sum_{\{i,j\} \in E} h_{ij} + \sum_{i \in V} h_i \text{ with } h_i = \mathbf{B}_i \mathbf{S}_i \text{ and} \quad (\text{S9})$$

$$h_{ij} = J (S_i^x S_j^x + S_i^y S_j^y) - \kappa_{ij} D (S_i^x S_j^y - S_i^y S_j^x) + \Delta S_i^z S_j^z,$$

where $S^{x/y/z} = \hbar \sigma^{x/y/z} / 2$ with the Pauli matrices $\sigma^{x/y/z}$. Suppose that a product state $|\Psi\rangle$ is an eigenstate of the Hamiltonian (S9), i.e., $H|\Psi\rangle = \varepsilon|\Psi\rangle$. We want to derive constraining relations for the product states that are equivalent to them solving the eigenvalue equation. To that end, we parameterize the product state in terms of angles ϑ_i and φ_i . Any product state can be generated by local rotations from a reference state $|\Omega\rangle \equiv \otimes_{i \in V} |\uparrow\rangle_i$ by

$$|\Psi(\boldsymbol{\vartheta}, \boldsymbol{\varphi})\rangle = U(\boldsymbol{\vartheta}, \boldsymbol{\varphi})|\Omega\rangle = \left(\prod_{i \in V} U_i(\vartheta_i, \varphi_i) \right) |\Omega\rangle, \quad (\text{S10})$$

where $U_i(\vartheta_i, \varphi_i) = e^{-\frac{i}{\hbar} \varphi_i S_i^z} e^{-\frac{i}{\hbar} \vartheta_i S_i^y}$, we abbreviate $U_i = U_i(\vartheta_i, \varphi_i)$ and $U = U(\boldsymbol{\vartheta}, \boldsymbol{\varphi})$. In this parameterization, $|\Psi(\boldsymbol{\vartheta}, \boldsymbol{\varphi})\rangle$ being an eigenstate of H is equivalent to $|\Omega\rangle$ being an eigenstate of $\tilde{H} = U^\dagger H U$. The constraints on the angles and hence the product eigenstates are derived by acting with \tilde{H} and requiring that $|\Omega\rangle$ must be an eigenstate of \tilde{H} .

$$\tilde{H} = U^\dagger H U = \sum_{\{i,j\} \in E} U_j^\dagger U_i^\dagger h_{ij} U_i U_j + \sum_{i \in V} U_i^\dagger h_i U_i, \quad (\text{S11})$$

$$\tilde{H}(\boldsymbol{\vartheta}, \boldsymbol{\varphi})|\Omega\rangle = \varepsilon(\boldsymbol{\vartheta}, \boldsymbol{\varphi})|\Omega\rangle + \sum_{i \in V} \lambda_i(\boldsymbol{\vartheta}, \boldsymbol{\varphi})|i\rangle + \sum_{\{i,j\} \in E} \mu_{ij}(\boldsymbol{\vartheta}, \boldsymbol{\varphi})|i,j\rangle. \quad (\text{S12})$$

$|i\rangle$ and $|j,k\rangle$ are the states with all spins up except for a single or two spins down on vertices i and j,k , respectively. These are the only basis states appearing after acting on the vacuum with \tilde{H} due to U preserving the locality of the interaction terms in the Hamiltonian. Since $|\Omega\rangle$, $|i\rangle$ and $|j,k\rangle$ are linearly independent, $|\Omega\rangle$ is an eigenvector of \tilde{H} (and $|\Psi(\boldsymbol{\vartheta}, \boldsymbol{\varphi})\rangle$ an eigenvector of H) if and only if

$$\lambda_i(\boldsymbol{\vartheta}, \boldsymbol{\varphi}) = 0 \quad \forall i \in V, \quad (\text{S13})$$

$$\mu_{ij}(\boldsymbol{\vartheta}, \boldsymbol{\varphi}) = 0 \quad \forall \{i,j\} \in E. \quad (\text{S14})$$

These equations are a special case of results derived in [21] since we impose a uniform interaction strength for all edges and a $U(1)$ -symmetry, i.e., rotational symmetry about the z -axis, on the quadratic terms in the Hamiltonian. We want to give explicit expressions for Eqs. (S13) and (S14). Acting on $|\Omega\rangle$, the contributions in Eq. (S11) that are quadratic in the spin operators yield

$$\begin{aligned} & \frac{4}{\hbar^2} U_j^\dagger U_i^\dagger h_{ij} U_i U_j |\Omega\rangle \\ &= (\cos(\vartheta_i) \cos(\vartheta_j) \Delta + \sin(\vartheta_i) \sin(\vartheta_j) (\cos(\varphi_i - \varphi_j) J + \sin(\varphi_i - \varphi_j) \kappa_{ij} D)) |\Omega\rangle \\ &+ (\cos(\vartheta_i) \sin(\vartheta_j) (\cos(\varphi_i - \varphi_j) J + \sin(\varphi_i - \varphi_j) \kappa_{ij} D) - \sin(\vartheta_i) \cos(\vartheta_j) \Delta - i \sin(\vartheta_j) (\sin(\varphi_i - \varphi_j) J - \cos(\varphi_i - \varphi_j) \kappa_{ij} D)) |i\rangle \\ &+ (\cos(\vartheta_j) \sin(\vartheta_i) (\cos(\varphi_i - \varphi_j) J + \sin(\varphi_i - \varphi_j) \kappa_{ij} D) - \sin(\vartheta_j) \cos(\vartheta_i) \Delta + i \sin(\vartheta_i) (\sin(\varphi_i - \varphi_j) J - \cos(\varphi_i - \varphi_j) \kappa_{ij} D)) |j\rangle \\ &+ (\sin(\vartheta_i) \sin(\vartheta_j) \Delta + (\cos(\vartheta_i) \cos(\vartheta_j) - 1) (\cos(\varphi_i - \varphi_j) J + \sin(\varphi_i - \varphi_j) \kappa_{ij} D)) |i,j\rangle \\ &+ i ((\cos(\vartheta_i) - \cos(\vartheta_j)) (\sin(\varphi_i - \varphi_j) J - \cos(\varphi_i - \varphi_j) \kappa_{ij} D)) |i,j\rangle. \end{aligned} \quad (\text{S15})$$

The terms linear in the spin operators yield

$$\begin{aligned} \frac{2}{\hbar} U_i^\dagger h_i U_i |\Omega\rangle &= (\sin(\vartheta_i) \cos(\varphi_i) B_i^x + \sin(\vartheta_i) \sin(\varphi_i) B_i^y + \cos(\vartheta_i) B_i^z) |\Omega\rangle \\ &+ (\cos(\vartheta_i) \cos(\varphi_i) B_i^x + \cos(\vartheta_i) \sin(\varphi_i) B_i^y - \sin(\vartheta_i) B_i^z - i (\sin(\varphi_i) B_x - \cos(\varphi_i) B_y)) |i\rangle. \end{aligned} \quad (\text{S16})$$

As indicated in Eq. (S12), the orthonormality of $|\Omega\rangle$, $|i\rangle$ and $|i, j\rangle$ implies that $|\Psi(\boldsymbol{\vartheta}, \boldsymbol{\varphi})\rangle$ is an eigenstate if and only if the terms proportional to the $|i\rangle$ and $|i, j\rangle$ basis states vanish. The term proportional to $|\Omega\rangle$ gives the eigenenergy

$$\begin{aligned} \varepsilon(\boldsymbol{\vartheta}, \boldsymbol{\varphi}) &= \frac{\hbar^2}{4} \sum_{\{i,j\} \in E} (\cos(\vartheta_i) \cos(\vartheta_j) \Delta + \sin(\vartheta_i) \sin(\vartheta_j) (\cos(\varphi_i - \varphi_j) J + \sin(\varphi_i - \varphi_j) \kappa_{ij} D)) \\ &+ \frac{\hbar}{2} \sum_{i \in V} (\sin(\vartheta_i) \cos(\varphi_i) B_i^x + \sin(\vartheta_i) \sin(\varphi_i) B_i^y + \cos(\vartheta_i) B_i^z). \end{aligned} \quad (\text{S17})$$

The terms proportional to $|i\rangle$ yield the equations $\lambda_i(\boldsymbol{\vartheta}, \boldsymbol{\varphi}) = 0$ that eventually give rise to the vertex rule of the main text. Separated into real and imaginary part these equations read

$$\begin{aligned} \frac{\hbar}{2} \sum_{j \in V: \{i,j\} \in E} (\cos(\vartheta_i) \sin(\vartheta_j) (\cos(\varphi_i - \varphi_j) J + \sin(\varphi_i - \varphi_j) \kappa_{ij} D) - \sin(\vartheta_i) \cos(\vartheta_j) \Delta) \\ = -\cos(\vartheta_i) \cos(\varphi_i) B_i^x - \cos(\vartheta_i) \sin(\varphi_i) B_i^y + \sin(\vartheta_i) B_i^z, \end{aligned} \quad (\text{S18})$$

$$\frac{\hbar}{2} \sum_{j \in V: \{i,j\} \in E} \sin(\vartheta_j) (\sin(\varphi_i - \varphi_j) J - \cos(\varphi_i - \varphi_j) \kappa_{ij} D) = \cos(\varphi_i) B_i^y - \sin(\varphi_i) B_i^x. \quad (\text{S19})$$

The sums on the left-hand side run over the set of all nearest neighbors j of the vertex i . The terms proportional to $|i, j\rangle$ result in ‘‘edge equations’’ containing the constraints on the relative angles between two adjacent spins.

$$\begin{aligned} \sin(\vartheta_i) \sin(\vartheta_j) \Delta + (\cos(\vartheta_i) \cos(\vartheta_j) - 1) (\cos(\varphi_i - \varphi_j) J + \sin(\varphi_i - \varphi_j) \kappa_{ij} D) &= 0, \\ (\cos(\vartheta_i) - \cos(\vartheta_j)) (\sin(\varphi_i - \varphi_j) J - \cos(\varphi_i - \varphi_j) \kappa_{ij} D) &= 0. \end{aligned} \quad (\text{S20})$$

The terms in the Hamiltonian (S11) describing the coupling to magnetic fields add terms proportional to $|\Omega\rangle$ and $|i\rangle$. This leads to a Zeeman shift $\sum_{i \in V} \langle \mathbf{S}_i \rangle_{\Psi} \cdot \mathbf{B}_i$ of the energies and a source term in the vertex rule but does not affect the edge equations. In the easy-plane case discussed in the main text, including magnetic fields modifies the vertex equations (S18) and (S19) in the following way

$$\langle \dot{S}_i^z \rangle = \sin(\Theta) \left(\frac{\sin(\Theta) \sin(\gamma) \hbar^2 J}{4 \cos(\delta)} \sum_{j \in V: \{i,j\} \in E} \sigma_{ij} + \frac{\hbar B_i^x}{2} \sin(\varphi_i) - \frac{\hbar B_i^y}{2} \cos(\varphi_i) \right) = 0 \text{ and} \quad (\text{S21})$$

$$(\langle \mathbf{S}_i \rangle_{\Psi} \times (\langle \mathbf{S}_i \rangle_{\Psi} \times \mathbf{B}_i))_z = \frac{\hbar^2}{4} \sin(\Theta) (\cos(\Theta) \cos(\varphi_i) B_i^x + \cos(\Theta) \sin(\varphi_i) B_i^y - \sin(\Theta) B_i^z) = 0. \quad (\text{S22})$$

The energy is

$$\varepsilon = \frac{\hbar^2}{4} \Delta |E| + \sum_{i \in V} \langle \mathbf{S}_i \rangle_{\Psi} \cdot \mathbf{B}_i. \quad (\text{S23})$$

Easy-axis case

In the main text, we claim that in the easy-axis case in absence of magnetic fields, there are no other product eigenstates than the fully polarized states with all spins up or down. This follows from deriving the constraints on the relative angles as done for the easy-plane case. The angles of neighboring spins obey $\varphi_i - \varphi_j = \kappa_{ij} \delta$ and $\tan(\vartheta_i/2) / \tan(\vartheta_j/2) = \exp(\sigma_{ij} \gamma)$ with the sign $\sigma_{ij} = -\sigma_{ji} = \pm 1$. In addition, the signs in the ϑ -constraint sum to $\sum_{j \in V: \{i,j\} \in E} \sigma_{ij} = 0$ at each vertex i . Note that, as a consistency condition, the signs in the ϑ -constraint add to zero along every circuit $\Gamma \subset E$ in the graph and $\sum_{\{i,j\} \in \Gamma} \kappa_{ij} \delta \equiv 0 \pmod{2\pi}$. The vertex rule implies that the underlying graph is an Euler graph to allow for non-trivial product eigenstates. Any choice of an Euler orientation gives rise to an Euler circuit such that σ_{ij} is uniform along the circuit. This implies that the angles θ increase strictly monotonously along the Euler circuit since $\gamma > 0$. In particular, the relative changes in θ do not sum to zero violating the circuit rule for the easy-axis case. Hence, non-trivial product eigenstates do not exist in this case. However, including magnetic fields allows for fine-tuning of the vertex rule and the existence of non-trivial product eigenstates. In this case, the energy of the product eigenstates is

$$\varepsilon(\boldsymbol{\vartheta}) = \frac{\hbar^2 J}{4 \cos(\delta)} \sum_{\{i,j\} \in E} (\cos(\vartheta_i) \cos(\vartheta_j) \cos(\gamma) + \sin(\vartheta_i) \sin(\vartheta_j)) + \sum_{i \in V} \langle \mathbf{S}_i \rangle_{\Psi} \cdot \mathbf{B}_i. \quad (\text{S24})$$

Product eigenstates in the XX model on a square lattice

In this section, we provide further information for the XX model ($\gamma = \pi/2$, $\delta = 0$) on a square lattice with open boundaries. First, we determine all Kirchhoff orientations. Kirchhoff's rules and Fig. 2a imply that the edges of the outermost plaquettes have orientations forming vortices around these plaquettes, i.e., the arrows go around the plaquette either clockwise or counterclockwise. We claim that a choice of the plaquette orientations, clockwise or counter-clockwise, for the N leftmost and M bottommost plaquettes uniquely determines a valid Kirchhoff orientation. This follows from considering a minimal square lattice, see the (2, 2) case in Tab. SI, with three corner plaquettes having a prechosen circular orientation. From Kirchhoff's rules, it follows by combinatorics that this uniquely determines a valid Kirchhoff orientation. Now, the general lattice orientation can be determined by repeatedly applying the minimal lattice result starting from the bottom left corner of the lattice. This results in 2^{N+M-1} different Kirchhoff orientations.

From the Kirchhoff orientations, we can generate product eigenstates. Fixing global angles Φ and Θ , e.g., $\Phi = 0$ and $\Theta = \pi/2$ for the bottommost spin on the left boundary, i.e., it pointing in the x -direction, these eigenstates have the following form. Choosing a vortex orientation is equivalent to choosing a direction of the spins on the boundary vertices of degree 2. On the left boundary, they can either point in $+x$ or $-x$ -direction, and on the bottom in the $+y$ or $-y$ -direction. Spins in the same row or column as the boundary spin are determined by the anti-aligned order. Note that this is independent for each row and column. Also, since two product states are orthogonal if and only if at one site the spins point in opposite directions, the constructed product eigenstates are all orthogonal. This gives a lower bound for the eigenspace degeneracy of 2^{N+M-1} which is exponential in the length of the boundary. The total Hilbert space's dimension is $2^{N(M+1)+(N+1)M}$ and hence exponential in the area of the lattice. The so far constructed product eigenstates do not span the full eigenspace of product eigenstates, we have yet to consider the continuous degrees of freedom Φ and Θ . This eigenspace is spanned either by varying the global angles Φ and Θ or, as described in the main text, by the Θ - and Φ -derivatives of the product states in a single point (Φ, Θ) . However, the linear hull of all product eigenstates does not exhaust the total eigenspace degeneracy for states with the same eigenenergy as the product eigenstates. There is further degeneracy not stemming from product eigenstates or derived states such as the derivatives or projections onto eigenspaces of S^z , see Tab. SI. The same was observed for the kagome lattice on a torus in [24]. Nevertheless, numerics indicate that this degeneracy coincides with the appearance of product eigenstates.

Lower bound for the degeneracy of the ε -space

The estimate above for a lower bound on the dimension of the product eigenspace can be generalized for graphs with anisotropy angles $\gamma = \pi/(2n)$ with n a positive integer and an arbitrary δ . There the number of Kirchhoff orientations gives a lower bound on the product eigenspace degeneracy. Suppose that $\Phi = 0$ and $\Theta = \pi/2$. Now given two Kirchhoff orientations σ and σ' , the corresponding product eigenstates $|\psi\rangle$ and $|\psi'\rangle$ are orthogonal if and only if there is a vertex i such that $\varphi_i - \varphi'_i \equiv \pi \pmod{2\pi}$. This follows from the general formula for the scalar product of two product states

$$\langle \Psi(\vartheta', \varphi') | \Psi(\vartheta, \varphi) \rangle = \prod_{i \in V} \left(\cos\left(\frac{\vartheta'_i}{2}\right) \cos\left(\frac{\vartheta_i}{2}\right) e^{i\frac{\varphi'_i - \varphi_i}{2}} + \sin\left(\frac{\vartheta'_i}{2}\right) \sin\left(\frac{\vartheta_i}{2}\right) e^{-i\frac{\varphi'_i - \varphi_i}{2}} \right), \quad (\text{S25})$$

which simplifies to $\langle \Psi(\vartheta', \varphi') | \Psi(\vartheta, \varphi) \rangle = \prod_{i \in V} \cos((\varphi'_i - \varphi_i)/2)$ for $\vartheta_i = \vartheta'_i = \Theta = \pi/2$. Since every Kirchhoff orientation is also an Euler orientation, there exists a directed circuit Γ that contains all edges in E whose orientation is induced by σ . From the circuit rule it follows that $\sum_{\{j,k\} \in \Gamma} (\sigma_{jk} - \sigma'_{jk}) \gamma \equiv 2m\gamma \equiv 0 \pmod{2\pi}$ with m the number of edges where σ and σ' differ. Because $\sigma \neq \sigma'$, we have $m = 2nk$ for some positive integer k . In particular, we can find a vertex i such that there are exactly n edges along Γ where σ and σ' differ between the vertices 1 and i . Then, $\varphi_i - \varphi'_i = 2n\gamma = \pi$ and the assertion follows.

Product eigenstates in a circular chain

In this section, we give details on product eigenstates in spin chains that are helices and give the degeneracy of their eigenspaces. For an XXZ Heisenberg quantum spin 1/2 chain of length N with periodic boundary conditions, the determining rules for the product eigenstates simplify significantly. The circuit rule reduces to a periodic closure

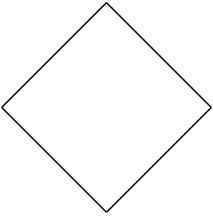
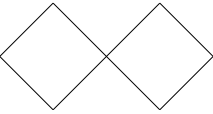
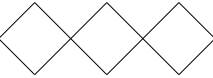
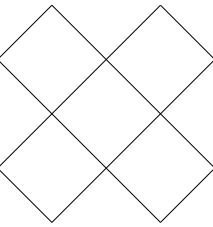
N	M	Graph	Orientations	Product Eigenstate Degeneracy	Total Degeneracy	Hilbert Space Dim.
1	1		2	8	10	16
1	2		4	24	44	128
1	3		8	64	234	1024
2	2		8	80	280	4096

TABLE SI. Degeneracy of the subspace spanned by the product eigenstates on the square lattice ($\Delta = D = 0$). N is the number of rows and M is the number of columns of the lattice. The number of orientations permissible with the product eigenstate equations is 2^{N+M-1} (fourth column) and the total Hilbert space dimension is $2^{N(M+1)+M(N+1)}$ (seventh column). The degeneracy of the product eigenstates is given in the fifth column, and further, the total degeneracy of the eigenspace with energy equal to the product eigenstates' energy, the ε -space, is depicted in the sixth column. The latter is determined by exact diagonalization (LAPACK) neglecting energy differences below $10^{-8}|J|$.

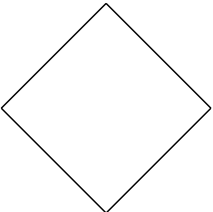
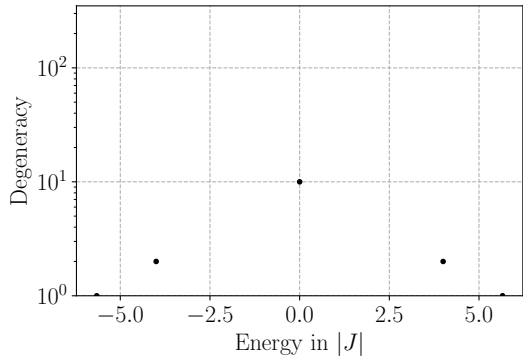
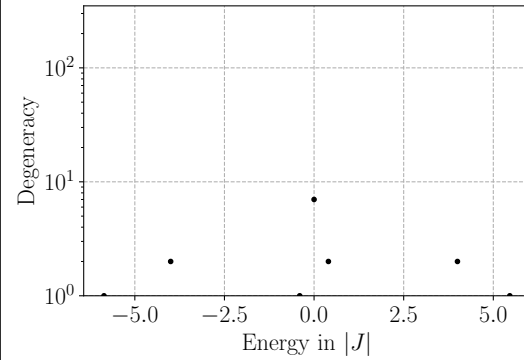
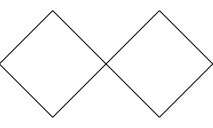
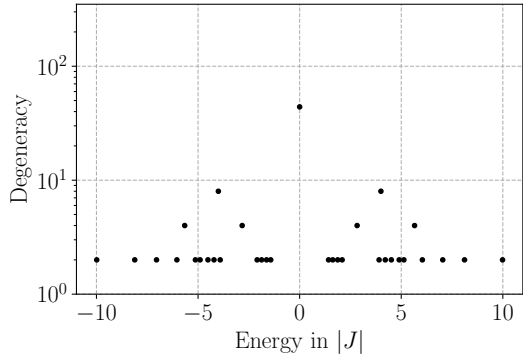
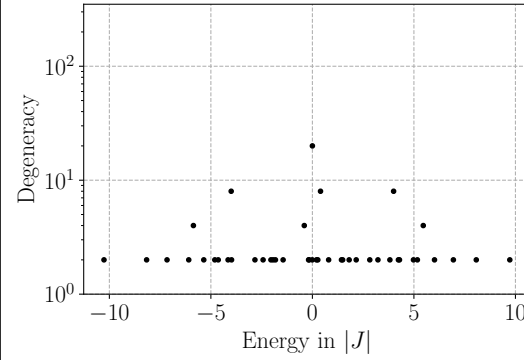
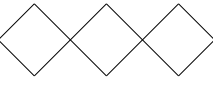
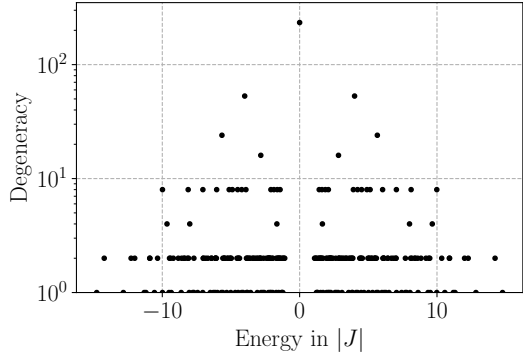
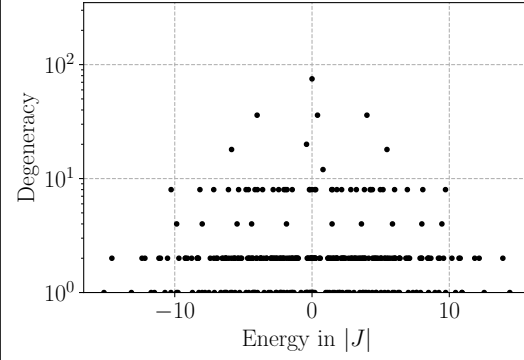
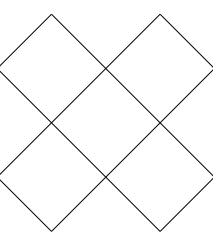
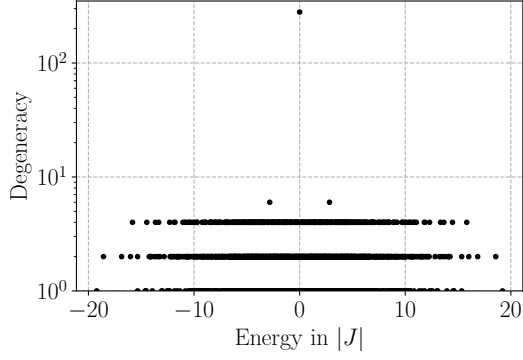
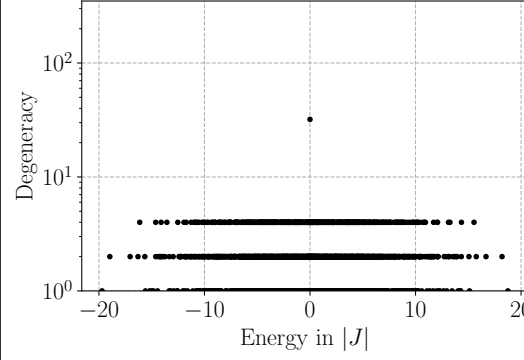
N	M	Graph	Degenerate Eigenspaces at $\Delta = 0$	Degenerate Eigenspaces at $\Delta = 0.1J$
1	1			
1	2			
1	3			
2	2			

TABLE SII. Degeneracy of the eigenspaces of the XX model on the square lattice as a function of energy. The degeneracy is determined by exact diagonalization (LAPACK) neglecting energy differences below $10^{-8}|J|$ and depicted for two different values of the anisotropy $\Delta = 0$ and $\Delta = 0.1J$ ($D = 0$ in both cases). We observe a massive reduction in degeneracy of the central eigenspace that accommodates the product eigenstates for $\Delta = 0$ when going to $\Delta = 0.1J$.

Δ/J	γ	$N=2$	$N=3$	$N=4$	$N=5$	$N=6$	$N=7$	$N=8$	$N=9$	$N=10$	$N=11$	$N=12$
1	0	3	4	5	6	7	8	9	10	11	12	13
-1	π	3		5		7		9		11		13
$-\frac{1}{2}$	$\frac{2\pi}{3}$		6			12			18(24)			24(48)
0	$\frac{\pi}{2}$			8(10)				16(60)				24(386)
$\frac{\sqrt{5}-1}{4}$	$\frac{2\pi}{5}$				10					20		
$\frac{1}{2}$	$\frac{\pi}{3}$					12						24(48)
$\cos\left(\frac{2\pi}{7}\right)$	$\frac{2\pi}{7}$						14					
$\frac{1}{\sqrt{2}}$	$\frac{\pi}{4}$							16				
$\cos\left(\frac{2\pi}{9}\right)$	$\frac{2\pi}{9}$								18			
$\frac{\sqrt{5}+1}{4}$	$\frac{\pi}{5}$									20		
$\cos\left(\frac{2\pi}{11}\right)$	$\frac{2\pi}{11}$										22	
$\frac{\sqrt{3}}{2}$	$\frac{\pi}{6}$											24

TABLE III. Dimension of the subspace spanned by product eigenstates of the linear spin chain with periodic boundary conditions for different critical values of the anisotropy angle γ and $\delta = 0$. The results are obtained from exact diagonalization (LAPACK). The dimension of the total subspace of all eigenstates of the same energy as the product eigenstates is denoted in brackets if it differs from the degeneracy due to the product eigenstates. Two orthogonal eigenstates are considered to be of equal energy if their energy differs by $10^{-8}|J|$.

condition $\gamma N \equiv 0 \pmod{2\pi}$ and the change of relative ϕ -angle must be constant along the chain resulting in two different kinds of helices [12–14] and were observed experimentally [20]. Their explicit form is

$$|\Psi^\pm(\Theta, \Phi)\rangle = \bigotimes_{j=1}^N \left(\cos\left(\frac{\Theta}{2}\right) e^{-i\frac{\Phi \pm j\gamma}{2}} |\uparrow\rangle_j + \sin\left(\frac{\Theta}{2}\right) e^{i\frac{\Phi \pm j\gamma}{2}} |\downarrow\rangle_j \right). \quad (\text{S26})$$

We note that the XXZ Heisenberg chain is integrable by means of the Bethe ansatz which allows, in principle, to get all eigenstates of the systems. The existence of these phantom helices is obscured in the standard formulation of the Bethe ansatz, where, the $U(1)$ -symmetry is exploited by performing the Bethe ansatz separately in the eigenspaces of $\sum_{j=1}^N S_j^z$. The phantom helices, though, have non-zero weight in more than one eigenspace of these eigenspaces. Phantom helices can be understood as solutions built from zero-modes acting on the pseudo-vacuum state. They play a prominent role in the chiral reformulation of the Bethe ansatz [12–14]. We investigated the degeneracy of the subspace spanned by the phantom helices of the XXZ chain by means of exact diagonalization for chain lengths up to $N = 12$, see Tab. SIII. We find that the degeneracy scales linearly in N . Further, we find that the degeneracy due to the phantom helices generically exhausts the degeneracy of the full subspace of the same energy as the phantom helices except for few cases.